



Article

Experimental Study on Sensitivity of Porosity to Pressure and Particle Size in Loose Coal Media

Chenghao Zhang ¹, Nong Zhang ^{1,*}, Dongjiang Pan ² , Deyu Qian ^{1,*} , Yanpei An ¹, Yuxin Yuan ¹, Zhe Xiang ¹ and Yang Wang ^{1,3}

¹ Key Laboratory of Deep Coal Resource Mining, Ministry of Education of China, School of Mines, China University of Mining and Technology, Xuzhou 221116, China; zhangchenghao421@126.com (C.Z.); anyanpei@cumt.edu.cn (Y.A.); yuanyuxin@cumt.edu.cn (Y.Y.); xiangzhe@cumt.edu.cn (Z.X.); TB15020024B0@cumt.edu.cn (Y.W.)

² State Key Laboratory of Shield Machine and Boring Technology, China Railway Tunnel Group Co., Ltd., Zhengzhou 450001, China; cumtpdj@163.com

³ School of Public Policy and Urban Affairs, College of Social Sciences and Humanities, Northeastern University, Boston, MA 02115, USA

* Correspondence: zhangnong@126.com (N.Z.); qian@cumt.edu.cn (D.Q.); Tel.: +86-136-0521-0567 (N.Z.); Tel.: +86-152-5201-6098 (D.Q.)

Received: 8 June 2018; Accepted: 27 August 2018; Published: 29 August 2018



Abstract: A new experimental method for characterizing the porosity of loose media subjected to overburden pressure is proposed based on the functional relationships between porosity, true density, and bulk density. This method is used to test the total porosity of loose coal particles from the Guobei coal mine in Huaibei mining area, China, in terms of the influence of pressure and particle size on total porosity. The results indicate that the total porosity of loose coal under 20 MPa in situ stress is about 10.22%. The total porosity and pressure obey an attenuated exponential function, while the total porosity and particle size obey a power function. The total porosity of the loose coal is greatly reduced and the sensitivity is high with increased pressure when stress levels are low (shallow burial conditions). However, total porosity is less sensitive to pressure at higher stress when burial conditions are deep. The effect of particle size on the total porosity reduction rate in loose coal is not significant, regardless of low- or high-pressure conditions; i.e., the sensitivity is low. The total porosity remains virtually unchanged as particle size changes when pressure exceeds 20 MPa. Overall, the sensitivity of total porosity to pressure is found to be significantly higher than sensitivity to particle size.

Keywords: loose media; coal; porosity; true density; bulk density; overburden pressure; particle size

1. Introduction

Porosity is one of the most important physical parameters used to characterize geological materials, including loose media which consists of a large number of particles basically belonging to the same order of magnitude, with voids between the particles and low mechanical strength, such as broken coal which has been subjected to tectonic stress failure, soil, and sand [1]. It is widely used in the field of mining and geotechnical engineering, as porosity is a primary control on material strength and behavior. The porosity of loose coal can be used to evaluate, among other things, the properties of coal reservoirs, the selection of grouting materials, the design of grouting parameters and the evaluation of grouting effects.

Mercury intrusion porosimetry (MIP), low-temperature nitrogen adsorption, and scanning electron microscopy (SEM) are the conventional methods of porosity testing [2–4]. Recently, some advanced techniques—such as nuclear magnetic resonance (NMR), computed tomography (CT), and

3D or 4D X-ray microscopes (XRM)—have also been applied to porosity testing [5–8]. However, these methods are mainly carried out at room temperature and ambient pressure, neglecting the key factor of overburden pressure for in situ geological materials. Although XRM is possible to measure pore structure parameters of subsurface rock systems at reservoir temperatures and pressures, it can only image mm-scale samples and it is ideal for resolving μm -scale processes [9,10]. To study the influence of pressure on porosity of cm-scale samples, some scholars have used automated porosity and permeability instruments or similar gas expansion principles to hold drilled core samples, and then apply different confining pressures and temperatures to study porosity variation [11,12], especially under different confining pressures. These core samples have typically consisted of low-permeability rocks and lump coal [13–22].

The above methods use drilled cores to test porosity of coal and other rock samples, but this is not possible for loose media that is pulverized and broken, in which drilling cores and press forming is not practicable. As such, it is difficult to study the influence of pressure and other factors on the porosity of loose media using the above-mentioned automated instruments, and some scholars tried to compress briquette and then testing porosity with porosity and permeability instruments [11,23–25]. There have also been very few experimental studies on the effects of particle size on the porosity of loose media [26–29] based on fractal theory or seepage experimental instruments.

In this paper, the research object of loose coal which is formed by tectonic stress failure, also called tectonically deformed coal [30], consists of a large number of broken particles, a type of loose media. Results are presented from the use of a true density tester and the use of a UTM5504 microcomputer-controlled electronic universal testing machine (Shenzhen Suns Technology Co., Ltd., Shenzhen, China) to accurately measure bulk density under overburden pressure. From this work, a suitable porosity testing method for loose media subjected to overburden pressure is proposed. It is based on the functional relationship between porosity, true density, and bulk density. This work also reveals the influence laws of different pressures and particle sizes on porosity.

2. Materials and Methods

2.1. Materials

Loose coal samples were collected from the haulage gateway of working face 8105-1 in coal seam 8₁ of the Guobei Coal Mine in the Huaibei mining area. The altitude of working face 8105-1 is between -683.6 m and -890.0 m , and the corresponding ground surface altitude varies from 29.6 m to 31.5 m . The structure of coal seam 8₁ is complex, as shown in Figure 1.

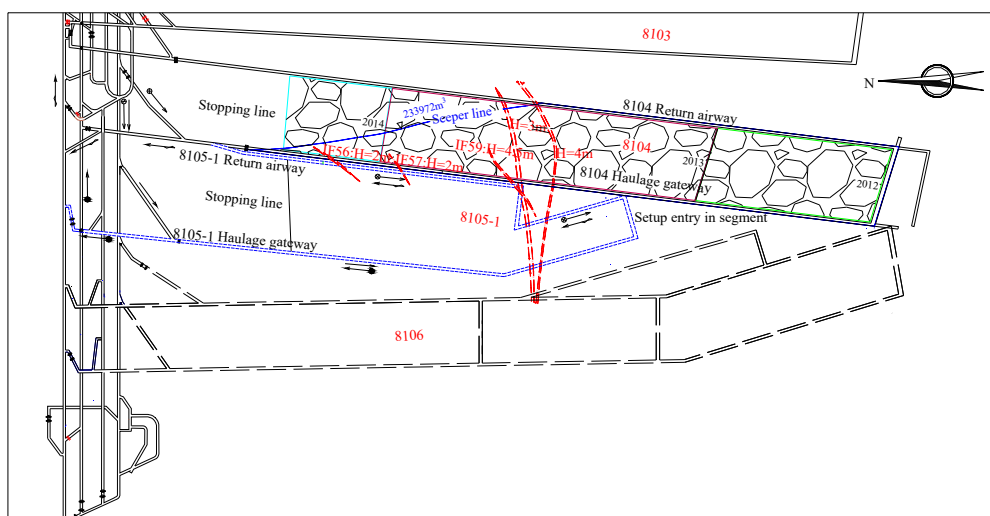


Figure 1. Position, production system, and geological structure of 8105-1 working face.

The coal body is grayish black to black, powdery to lumpy, partially scaly, with black streaks and a dull luster. It is a semi-bright coal. Detailed description and rock strata information were shown in Figure 2.

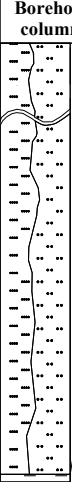




Rock strata	Borehole column	Thickness(m)	Lithological description
siltstone~ medium sandstone		15.59~29.26 22.02	Inner section: gray to light gray sandstone, continuous horizontal bedding. Outer section: grayish white, fine grained structure, local grain size is mainly composed of coarse siliceous, a small amount of dark minerals, parallel bedding, occasionally veined bedding, longitudinal oblique fracture.
		0.92~3.04 2.08	Gray to dark gray, flat fracture, muddy structure, partially silty, containing more plant fossil fragments.
		1.53~4.37 3.35	Black. Streak brown-brown black-black, powdery structure, glass luster-asphalt luster, endogenous fissures at the top and bottom are slightly developed, semi-bright coal dominated, occasionally bright coal, staggered-stepped fracture.
mudstone			
8 ₁ coal		0.83~1.50 1.19	Light gray to grayish black, blocky structure. Partially containing siltstone, containing more plant fossil fragments.
mudstone			
8 ₂ coal		1.87~4.75 3.29	Black, powder to broken structure, streaks brown to black, asphalt glass luster. Semi-dark to semi-light coal.

Figure 2. Borehole columnar section of coal seam.

To visually examine the pore spaces of the loose coal samples, the microstructure of the collected coal particles was observed using a SIGMA 300 field emission scanning electron microscope (Carl Zeiss, Oberkochen, Germany). The results were shown in Figure 3.

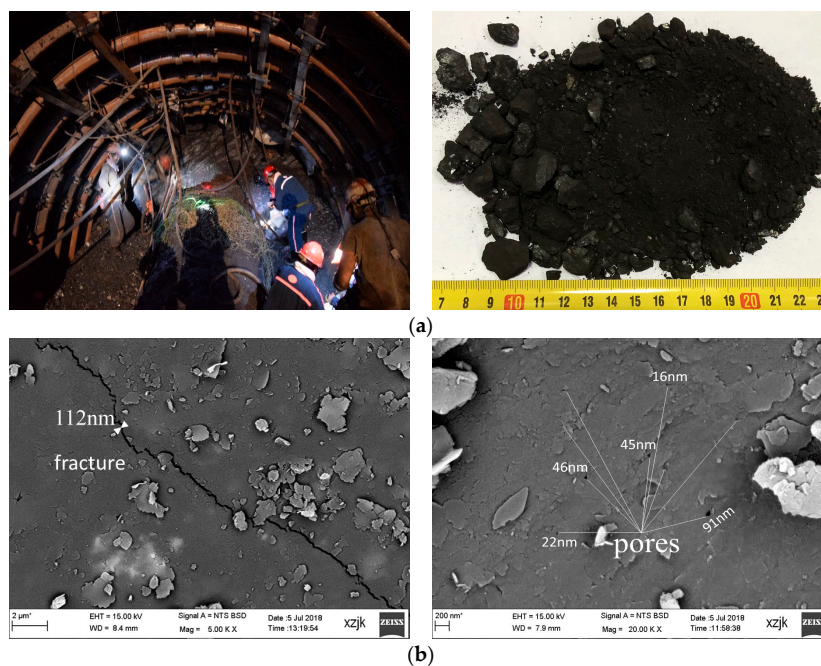


Figure 3. Cont.

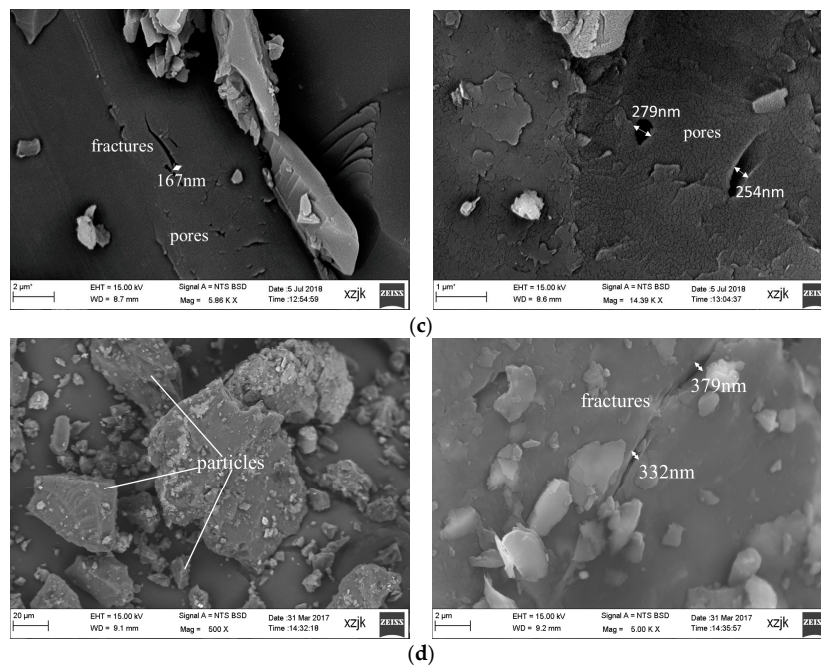


Figure 3. (a) On-site sampling photographs and (b–d) surface micromorphology of 5–15 mm, 2–5 mm, 0–2 mm coal particles from the 8₁ coal seam.

The sampling photographs and SEM images show that the loose coal body is composed of particles of different sizes, and the surfaces of the particles are further adhered to by tiny coal pieces. There are voids between the particles and when the coal particles are magnified, the microfractures and pores in the matrix are seen. The average labeled fracture width is about 247.5 nm, and the pore diameters focus on 16–45 nm.

The raw coal collected on-site from the mine is in the form of pulverized and fragmented coal. To understand the particle size distribution (PSD) of the raw coal and select the particle size gradient to study, initial sample screening (the mass of studied specimen was 2000 g) was performed, as shown in Table 1. Mesh diameter, grader retained percentage, and accumulated retained percentage in the table were used to plot the screening curve, as shown in Figure 4.

Table 1. Initial sample screening experiment data.

Mesh Diameter (mm)	Grader Retained Mass m_i (g)	Grader Retained Percentage ($m_i/2000$) (%)	Accumulated Retained Percentage (%)
31.5	0	0	0
16	124.77	6.2385	6.2385
9.5	131.25	6.5625	12.801
4.75	235.18	11.759	24.56
2.36	328.3	16.415	40.975
1.18	262.71	13.1355	54.1105
0.6	335.51	16.7755	70.886
0.3	189.61	9.4805	80.3665
0.15	183.05	9.1525	89.519
0.088	173.26	8.663	98.182
<0.088	15.98	0.799	98.981

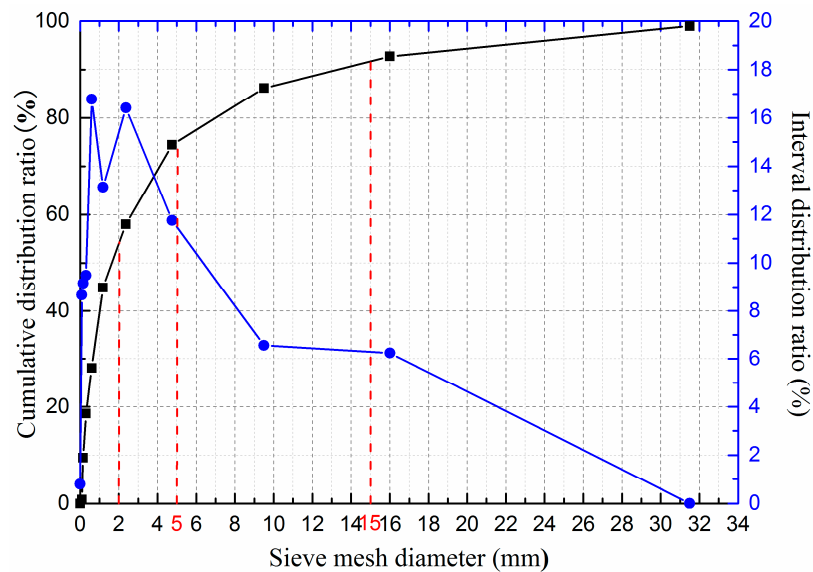


Figure 4. Cumulative and interval distribution curves of loose coal sample particle sizes.

Results of the initial screening show that coal particles >15 mm with very low distribution were not considered. Sieves with mesh diameters of 2, 5, and 15 mm were used for re-screening to obtain three particle size ranges of 0–2, 2–5, and 5–15 mm, which are similar to the particle size of three types of tectonically deformed coal, mylonitic coal (<1 mm), granulated coal (1–3 mm), and tectonically crushed coal (3–10 mm) after being broken by pressure [31,32], as shown in Figure 5. The above three size classes from the screening and raw coal (mixed particle sizes: 0–2 mm, 50%; 2–5 mm, 30%; 5–15 mm, 20%) were used in the porosity characterization and influencing factors tests.



Figure 5. Screened coal particles of three different particle size classes.

2.2. Methods

2.2.1. Porosity in the Particle Matrix

Porosity in the matrix of particles was characterized using the combined methods of mercury intrusion porosimetry (MIP) and low temperature nitrogen adsorption.

The MIP experiments were carried out using an Autopore 9510 Mercury Porosimeter (Micromeritics Instrument Corp., Norcross, GA, USA). This instrument can use mercury intrusion pressures from atmospheric pressure to 60,000 psi (414 MPa) and measure pore sizes in the 0.003–6 μm range with a $\pm 0.10\%$ transducer accuracy of full scale. The samples used was about 5–15 mm in size and dried at 110 $^{\circ}\text{C}$ for 24 h before the experiment.

The mercury porosimetry analysis technologies are based on the intrusion of mercury into aporous structure under stringently controlled pressures. They can capture numerous sample pore properties such as pore size distributions, total pore volume, or porosity. The porosity calculation formula is

$$n_p = V_1/V_2 \quad (1)$$

where n_p is the particle matrix porosity; V_1 is the pore volume (mercury volume intruded at the maximum experimental pressure attained, 414 MPa) and V_2 is the sample volume which can be derived by Equation (2)

$$V_2 = \{w_4 - [w_3 - (w_2 - w_1)]\} / \rho_{Hg} = (w_4 - w_3 + w_2 - w_1) / \rho_{Hg} \quad (2)$$

where ρ_{Hg} is the density of mercury at a certain temperature; w_1 is the mass of empty cell; w_2 is the mass of empty cell and sample; w_3 is the mass of mercury, empty cell and sample and after filling with mercury under a certain pressure; w_4 is the mass of mercury and empty cell after empty cell filled with mercury.

Due to compression of mercury, of the sample cell, and of the rest of the instrument components, but also of the sample itself, the mercury intrusion method will have a certain error, especially at higher mercury pressures [33,34]. Subtracting an empty cell run from an actual sample analysis is an effective means to correct compression of mercury and system components error (blank correction). For the problem of compressibility of coal under high pressure of mercury intrusion, low temperature nitrogen adsorption was used to instead of MIP to calculate the pore volume which was originally tested with mercury intrusion at high pressure.

The low temperature nitrogen adsorption experiments were carried out using a Micromeritics ASAP 2460 (Micromeritics Instrument Corp., Norcross, GA, USA) gas adsorption instrument. Samples were crushed to 250 μm and dried at 100 $^\circ\text{C}$ for 24 h to be used for low pressure isotherm analysis. After outgassing at 150 $^\circ\text{C}$ for 8 h, the N_2 gas isotherm adsorption measurements were carried out at 77 K (-196 $^\circ\text{C}$). The pore volume and pore size distribution can be obtained from the low temperature nitrogen adsorption experiments.

2.2.2. Total Porosity of Loose Coal

According to the China National Standard [35], the extended formula for calculating total porosity while under overburden pressure is

$$n_t = (1 - \rho_b / \rho) \times 100\% \quad (3)$$

where n_t is the total porosity of coal or rock (%); ρ_b is the bulk density of coal or rock, i.e., the ratio of mass to total volume of coal or rock (including the volume of skeleton and all pore spaces, g/cm^3) and ρ is the true density or mineral particle skeletal density of coal or rock (the ratio of mass to skeleton volume, not including the pore spaces, g/cm^3).

The test of true density (ρ) was done with the true density tester. The testing instrument was an AccuPyc 1330 Pycnometer (Micromeritics Instrument Corp., Norcross, GA, USA). The instrument uses the Archimedes principle of helium gas expansion. The molecular diameter of He is 0.26 nm, thus it can penetrate the smallest pores and irregular hollows in the surface of a sample. As a result, it is possible to obtain a skeleton volume very close to the true skeleton volume value, and the calculated true density is therefore a true reflection of the true density value of any given sample.

To determine bulk density (ρ_b) of coal samples at different pressures, the UTM5504 universal testing machine was used. The experimental equipment used and a schematic diagram of the method were shown in Figure 6.

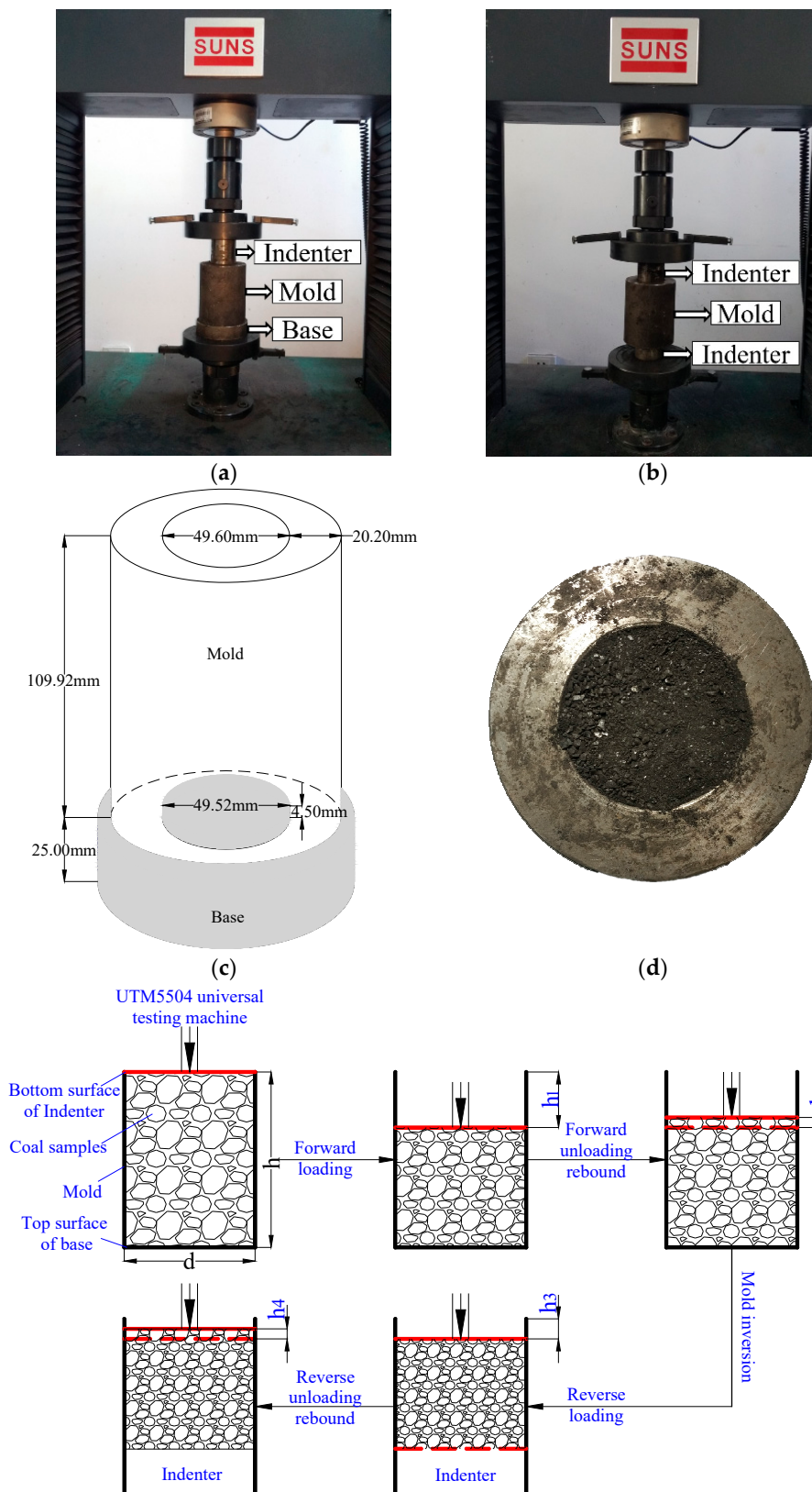


Figure 6. (a) Forward loading photograph; (b) reverse loading photograph; (c) mold schematic diagram; (d) schematic diagram of initial experimental coal samples; and (e) schematic diagram of the test apparatus and methodology for determining bulk density of coal at different pressures.

To accurately simulate the in situ state of pressure, the experiment was run in four stages:

- (1) Forward loading stage: A loading speed of 2 mm/min was used, and after the specified pressure (Determined according to the in situ stresses—5, 10, 15, 20, and 25 MPa—was selected in this test because the in situ stress of Guobei Coal Mine 8105-1 working face is 20 MPa) level was reached, the force applied was kept constant for 30 min. The loading time was referenced by some scholars' briquette compressing schemes [24,25,36,37]. The forward decreased displacement of indenter h_1 was automatically recorded by the testing machine. At each initial experiment, the coal sample should be filled with the mold, that is, the initial position of the bottom surface of the indenter was flush with the top of the coal briquette mold, as shown in Figure 6d. The purpose of the operation is to conveniently calculate the height of the coal sample after compressing. After this stage, $h_{\text{coal}} = h - h_1$. h is the height of the briquette mold excluding the base embedded in the mold.
- (2) Forward unloading rebound stage: The unloading speeds were set to 15 N/s corresponding to experimental pressures of 5 MPa, 30 N/s→10 MPa, 45 N/s→15 MPa, 60 N/s→20 MPa, and 75 N/s→25 MPa. The purpose is to keep the consistent unloading time at each pressure. When the force returned to zero, the compressed coal sample rebounded and the forward rebound amount of the coal sample h_2 was recorded.
- (3) Reverse loading stage: The briquette mold was reversed, and the pressure was applied continuously. The loading speed was set to 2 mm/min and after the specified pressure level (5, 10, 15, 20, and 25 MPa) was reached the applied force was kept constant for 30 min. The reverse loading parameters were exactly the same as the parameters in the forward loading stage. The reverse decreased displacement of indenter h_3 was recorded.
- (4) Reverse unloading rebound stage: The unloading speeds were set to 15 N/s corresponding to experimental pressures of 5 MPa, 30 N/s→10 MPa, 45 N/s→15 MPa, 60 N/s→20 MPa, and 75 N/s→25 MPa. When the reverse force returned to zero, the compressed coal sample rebounded and the reverse rebound amount h_4 was recorded.
- (5) The mold was again turned upside down and the next level of pressure was applied. The previous four stages were repeated to complete the next pressure level tests.

The bulk density of coal under different pressures was then calculated as shown in Equation (4).

$$\rho_b = \frac{m}{\pi(d/2)^2[h - (h_1 + h_3 - h_2)]} \quad (4)$$

where ρ_b is the bulk density of coal under a certain overburden pressure (g/cm^3); m is the mass in grams of the coal sample in the briquette mold (the coal sample filled the mold at the beginning of the test); and d is the inner diameter of the briquette mold (cm). The inner diameter used in this experiment was 4.960 cm.

The various heights and displacements are as follows: h is the height of the briquette mold (10.542 cm) excluding the base embedded in the mold; h_1 is the forward decreased displacement (cm) of the indenter under a certain overburden pressure; h_2 is the forward rebound amount (cm) of the coal sample when the overburden pressure returns to zero; and h_3 is the reverse decreased displacement (cm) of the indenter under a certain overburden pressure. The result of $h - (h_1 + h_3 - h_2)$ is the height of the compressed coal samples under each pressure.

It should be noted that Equation (4) applies to the calculation of the bulk density of the independently filling and compressing coal samples under each pressure level, but if the coal sample compression of a certain pressure level continues to circulate on the basis of the previous pressure level, when calculating the height of the compressed coal sample, it is necessary to subtract the influence of the reverse rebound amount h_4 of the previous pressure level. For example, in the experiment scheme of this article, when the pressure is 5 MPa, the bulk density can be calculated directly using Equation (4), but when 10 MPa, the reverse rebound amount h_4 of 5 MPa needs to be subtracted when

calculating the height of the compressed coal sample. Because the 10 MPa forward loading stage was followed by 5 MPa reverse unloading rebound stage.

In the bulk density experiment, the mass of the coal sample was measured using a precision balance (Yuyao Jiming Weighing Calibration Equipment Co., Ltd., Ningbo, China, JM-A20002, MAX = 2000 g, $d = 0.01$ g) and the height and inner diameter of the mold were measured using a Vernier caliper (Hangzhou Huafeng Big Arrow Tools Co., Ltd., Hangzhou, China, HF-8631215, MAX = 150 mm, $d = 0.01$ mm). The decreased displacement and rebound amount of the indenter were automatically recorded by the testing machine with a $0.04 \mu\text{m}$ displacement resolution. The maximum test force of the machine is 50 kN (resolution 1/500,000).

3. Results

3.1. Characterization of Total Porosity of Loose Coal

Total porosity refers to the ratio of the sum of the volume of all pore spaces in a rock sample to the volume of the sample. For loose coal, the total porosity consists of three parts: inter-particle voids, pores, and micro-fractures in the particle matrix.

The porosity of the loose coal matrix was obtained by mercury intrusion porosimetry and low temperature nitrogen adsorption. After testing the true density of the loose coal sample and the bulk density subjected to overburden pressure, the total porosity of the loose coal samples was determined from the functional interrelationships of total porosity, true density, and bulk density. Thus, the objective of accurately characterizing the porosity of loose coal which is multi-scale pore spaces (millimeter voids, micro-nano fractures and pores) was achieved.

3.1.1. True Density

The true densities of minerals in coal are much greater than the true densities of organic matter within coal. For example, the true densities of quartz, clay and pyrite are 2.15 , 2.40 , and 5.00 g/cm^3 , respectively. The average true density of minerals in coal is approximately 3.00 g/cm^3 , and the higher the inorganic mineral content, the higher the true density of the coal [38]. The associated mineral compositions of the coal samples were analyzed by the D8 ADVANCE X-ray diffractometer (Bruker AG, Karlsruhe, Germany), as shown in Figure 7.

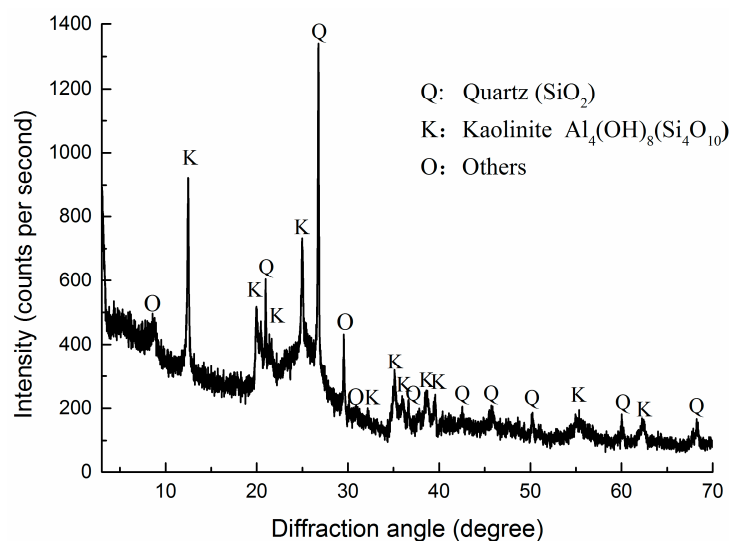


Figure 7. X-ray diffraction pattern of 8₁ coal sample.

Figure 7 shows that the coal sample collected in the experiment contained quartz, kaolinite, and other minerals, and the mineral contents were shown in Table 2.

Table 2. Results of quantitative analysis of 8₁ coal sample minerals.

Minerals	Quartz	Kaolinite	Others
Weight percentage	12.04%	9.47%	3.79%

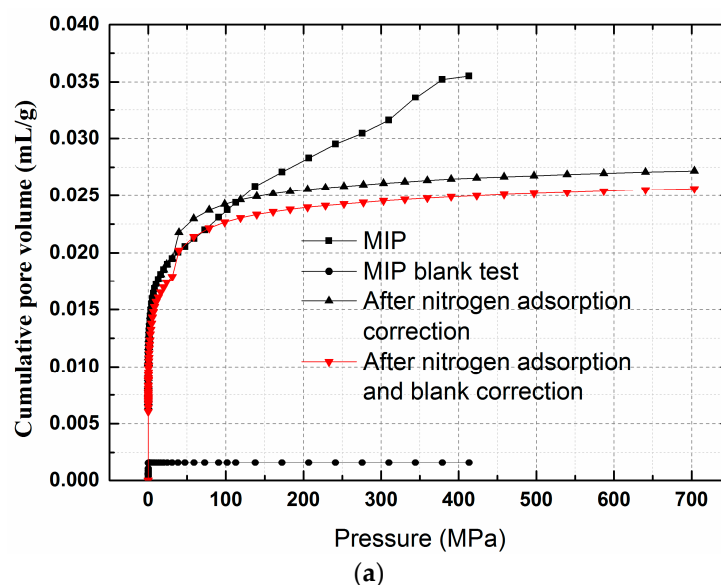
As a result, the true densities measured for different particle size of coal were different, as shown in Table 3. The difference in true density values of different coal particle sizes may be due to the different mineral contents.

Table 3. True densities of coal measured for different size classes of coal particles.

Size	0–2 mm	2–5 mm	5–15 mm	Raw Coal
True density	1.562 g/cm ³	1.632 g/cm ³	1.827 g/cm ³	1.636 g/cm ³

3.1.2. Porosity in the Particle Matrix

The matrix porosity of 5–15 mm samples from coal seam 8₁ determined from the combined test of MIP and low temperature nitrogen adsorption was 4.23%. With 50 nm as the demarcation point of MIP and low temperature nitrogen adsorption [39,40], volume data for pores (diameter > 50 nm) used MIP data, and pores (diameter < 50 nm) used low temperature nitrogen adsorption data. The comparison between combined methods and separate MIP was shown in Figure 8a. In the figure, in order to show the comparison and correction more intuitively, the pore diameter data of low temperature nitrogen adsorption was converted into mercury intrusion pressure. Cumulative porosity and porosity distribution curves after correction were shown in Figure 8b. The matrix porosity of this sample is mainly distributed as transitional pores (reference to Hodot pore grading [41]), with pore throat diameters in the range of a 20–40 nm, and 90–347 μm diameter fractures and pores (visible to naked eye) which have an order of magnitude size difference compared to the transitional pores are also evident. There are also few abrupt peaks on the porosity distribution curve which may be due to the randomness of the samples.

**Figure 8.** Cont.

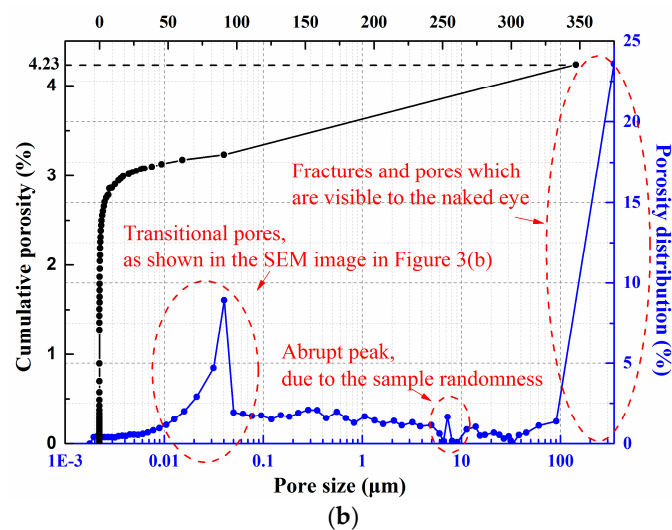


Figure 8. Results of pore space characterization using MIP and low temperature nitrogen adsorption: (a) pore volume and (b) porosity in the coal matrix.

3.1.3. Total Porosity of Loose Coal

The total porosity value was calculated by substituting the bulk density results and true density results into Equation (3). Results were shown in Figure 9. The actual depth (H) of the experimental sample collection site was about 800 m, based on the estimation of in situ stress ($\sigma = \gamma H$) where a value of 2.5 kN/m^3 was used for γ and the in situ stress at the sampling site was $\approx 20 \text{ MPa}$. The experimental results indicate a total porosity value of 10.22% for the sample from the 8_1 coal seam at 20 MPa.

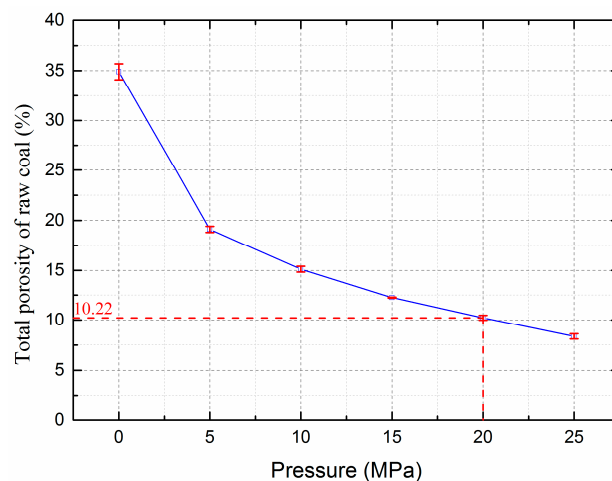


Figure 9. Curve of total porosity for a sample of coal from the 8_1 coal seam.

According to the MIP and low-temperature nitrogen adsorption data, the porosity in the matrix of particles from the 8_1 coal seam was approximately 4.23%. The remaining porosity of 5.99% for samples subjected to 20 MPa of overburden pressure was obtained from the inter-particle voids and the smaller pores (diameter $< 1.77 \text{ nm}$) not measurable with the low temperature nitrogen adsorption experiment. In this article, the single coal sample of 5–15 mm was used in the MIP experiment, so the porosity result from MIP experiment does not include inter-particle voids. It can also be seen from the mercury intrusion curve that there is no obvious inflection point at low pressure.

3.2. Effects of Pressure and Particle Size on Total Porosity

The research object loose coal (tectonically deformed coal) has different burial depths and degrees of fragmentation. Different overburden pressures applied to loose, raw coal particles will result in deformation, breaking, rearrangement, and other changes that will cause the total porosity to change significantly. In addition, under the same overburden pressure, the arrangement and staggered relationship of coals with different particle sizes may also result in different porosity. To test the effects of pressure and particle size on total porosity, the characteristics of in situ stress and particle sizes of raw coal have been combined, and total porosity has been determined for different pressure gradients (0, 5, 10, 15, 20, and 25 MPa) and different particle size classes (0–2, 2–5, and 5–15 mm). The experimental results obtained are described in the following three subsections.

3.2.1. Pressure Effects on Total Porosity

Changes in total porosity with increasing pressure for the specified particle size classes have been constructed as curves, with data points fitted and analyzed (Figure 10 and Table 4). These data show that as pressure increases, the pores between the particles gradually close and the total porosity decreases for each particle size class. When the pressure is low, the degree of decrease is greatest, and as pressure increases the degree of decrease is gradually reduced.

Additionally, the total porosity and pressure obey an attenuated exponential function (all curves have an R-square of $\approx 98\%$). That is, the total porosity decreases exponentially with increasing pressure. Regression analysis of the experimental results show that the relationship can be defined as

$$n_t = ae^{-b\sigma} + c \quad (5)$$

where n_t is the total porosity of loose coal at a given pressure (%), σ is the pressure (MPa), the sum of a and c represents the total porosity of loose coal when the pressure is 0 MPa (%), and b represents the compression coefficient (MPa^{-1}).

Finally, the decreases in total porosity for each particle size class are similar as pressure increases, and the curves steepen. A mixed particle sizes (such as raw coal) will reduce the rate of total porosity decrease as pressure increase, evident in the gentle slope of the curve. The raw coal has a relatively low porosity at low pressure. For example, compared with 5–15 mm particles, the porosity value of the raw coal under 0 MPa is 15.31% less, and the value under 5 MPa is 3% less. This is because the staggered arrangement of large and small coal particles in raw coal and small particles filled large voids.

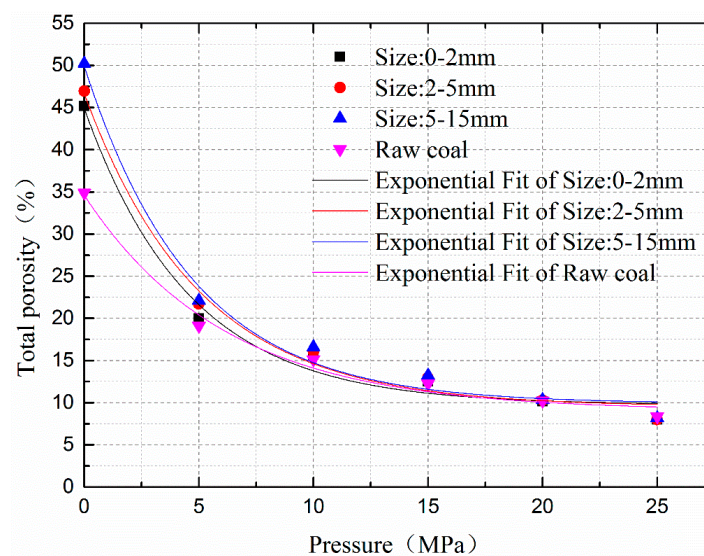


Figure 10. Curves of total porosity change with increasing pressure for specified particle size classes.

Table 4. Fitting formulae of total porosity for each particle size class.

Size	Fitting Formula	R-Square
0–2 mm	$n_t = 0.098 + 0.351e^{-0.217\sigma}$	0.97848
2–5 mm	$n_t = 0.095 + 0.371e^{-0.199\sigma}$	0.98336
5–15 mm	$n_t = 0.099 + 0.400e^{-0.211\sigma}$	0.98217
Raw coal	$n_t = 0.091 + 0.255e^{-0.162\sigma}$	0.98215

3.2.2. Particle Size Effects on Total Porosity

The study of loose coal particle size effects on total porosity includes two aspects: the initial particle size and the particle size of the compacted samples. The study of initial particle size has a reference value for the study of the influence of porosity on the physical and mechanical properties of coal by compressing coal samples with different porosity in the laboratory. The particle size of the compacted samples are the true particle size after laboratory or on-site compression, which truly reflects the relationship between the porosity and on-site tectonically deformed coal of different degrees of fragmentation. Using the cumulative PSD curve (Figure 4), the initial particle size D_{50} was selected as the average particle size of the segment. This is the particle size corresponding to 50% of the cumulative PSD in each segment of the three size classes. The fitting curve in Figure 4 shows that the D_{50} results for each segment are 0.54, 3.15, and 8.57 mm, respectively. From these data, it was possible to construct curves of total porosity change vs. initial particle size for each pressure interval, as shown in the line graph in Figure 11. The coal samples after each stage of loading screening was performed. Using the obtained particle size after loading, the curves of total porosity change vs. the particle size of the compacted samples were plotted, as shown in the histogram in Figure 11.

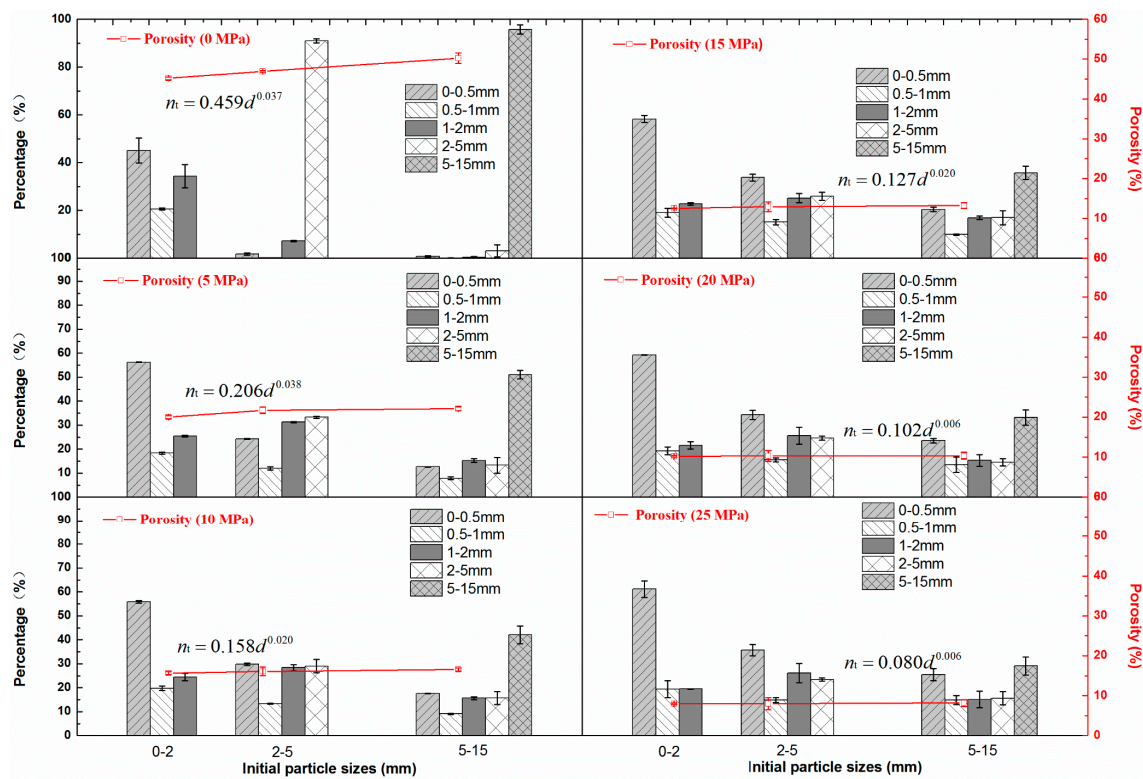


Figure 11. Curves of total porosity change vs. initial particle size and the particle size of the compacted samples.

The line graph curves show that, at each pressure, the total porosity increases with increasing initial particle size and, by fitting of the data points, the relationship between total porosity and initial particle size is shown to obey the power law

$$n_t = Ad^B \quad (6)$$

where n_t represents the total porosity; d represents the initial particle size and A and B are fitting constants.

The histograms show that the largest particles are gradually crushed and decreased as the pressure increase, and the degree of fragmentation is irregular. There is still a clear difference in particle size with the initial coal particles of 5–15, 2–5, and 0–2 mm subjected to the same pressure. Large initial particles correspond to low degree of on-site coal fragmentation.

Additionally, as pressure and initial particle size increases, the increased degree of total porosity undergoes a gradual decrease. When the pressure exceeds 20 MPa, the curve of initial particle size vs. total porosity approximates a straight line, indicating that the total porosity does not change with a change in initial particle size.

From the relationship between porosity and particle size of the compacted samples, it can be seen that the porosity of coal samples with low degree of fragmentation is larger than the coal samples with high degree of fragmentation, but the difference is small. As the overburden pressure increases, the difference gradually decreases. After 20 MPa, the difference tends to be zero. At this time, the porosity is considered to be independent of the degree of coal fragmentation.

3.2.3. Sensitivity of Total Porosity to Pressure and Particle Size

Evaluation of the sensitivity of total porosity to pressure and initial particle size is based on the use of total porosity reduction rate as the sensitivity parameter and a reference point with total porosity measured in coal in the 5–15 mm particle size range at a pressure of 0 MPa. The rate of change of total porosity with respect to the reference point at each pressure and initial particle size was defined as the total porosity reduction rate (Δn_t), as expressed in Equation (7). The greater the value of change in Δn_t as some other factor changes, the higher the sensitivity of total porosity to that factor, as

$$\Delta n_t = \frac{(n_0 - n_{ij})}{n_0} \times 100\% \quad (7)$$

where n_0 is the total porosity of coal samples in the 5–15 mm initial particle size range measured at 0 MPa pressure and n_{ij} is the total porosity measured for any particle size and pressure.

The reduction rate of total porosity for each initial particle size class and pressure was calculated according to Equation (7), and the results were shown in Table 5.

Table 5. Reduction rates of total porosity (Δn_t) for each particle size class and pressure.

Size Pressure	5–15 mm	2–5 mm	0–2 mm
	0 MPa	0	6.54%
5 MPa	55.96%	56.78%	60.18%
10 MPa	66.97%	67.96%	68.76%
15 MPa	73.64%	74.19%	75.04%
20 MPa	79.41%	79.55%	79.73%
25 MPa	83.74%	84.06%	84.06%

Table 5 shows that the total porosity of the loose coal is greatly reduced when the pressure is low (shallow burial conditions), and the sensitivity is high with respect to increasing pressure. Total porosity is less sensitive to pressure at higher stress levels (deep burial conditions). The change

in total porosity reduction rate is not significant in terms of initial particle size changes, regardless of whether the pressure conditions are low or high, and the sensitivity is low. Generally, the sensitivity of total porosity to pressure is significantly higher than sensitivity to initial particle size (corresponding to degree of on-site coal fragmentation).

4. Discussions

4.1. Comparison with the Method of Compressing Briquette and Testing Porosity

There are two main problems with the method of compressing briquette and then testing porosity: one problem is that the difficulties of forming and taking out the briquette at low pressure, and another problem is that the briquette has a large amount of rebound at high pressure. The rebound amount can be reflected by the time–displacement curves measured from the UTM5504 universal testing machine, as shown in Figure 12a. The curves show that there is rebound after loading and unloading at all pressure levels. As the pressure level increases, the amount of rebound gradually increases. Thus, the error related to the porosity testing method by briquette mentioned in the introduction under overburden pressure also increases. The comparison of porosity differences caused by errors were shown in Figure 12b. The total porosity is calculated by Equation (3). When calculating, the method of compressing briquette accounts for the reverse rebound amount (h_4), but the method proposed in this paper eliminates the impact of the reverse rebound amount, not counting.

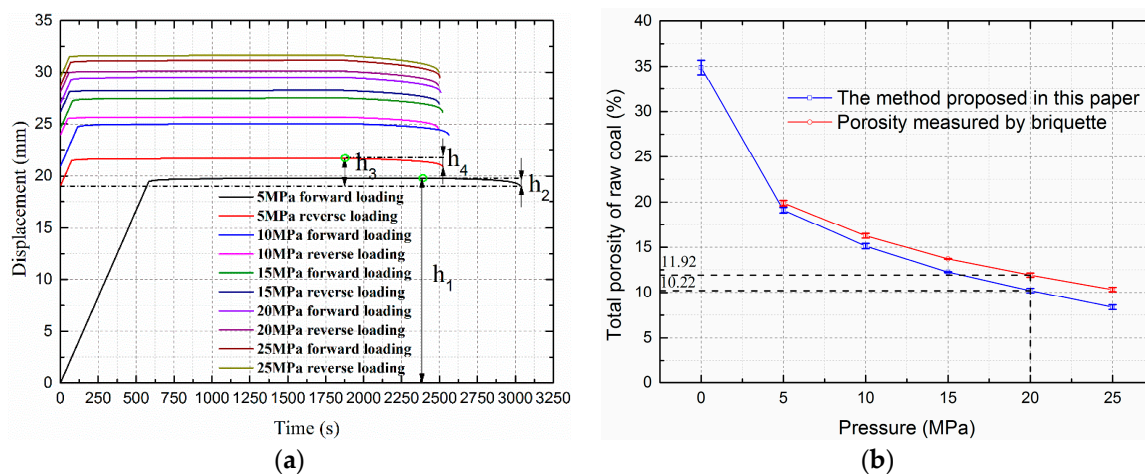


Figure 12. (a) Time–displacement curves determined during loading and unloading; and (b) comparison of porosity differences between the method of compressing briquette and then testing porosity and the method proposed in this paper.

4.2. Quality of Measurement Results

The true total porosity of on-site loose coal is difficult to measure or learn from relevant references, and the accuracy of this experiment cannot be quantitatively expressed. In these cases, uncertainty of measurement was usually used to evaluate the quality of measurement results [42,43]. It is the parameter, associated with the result of a measurement, that characterizes the dispersion of the values that could reasonably be attributed to the measurand. In most cases, a measurand is not measured directly, but is determined from other quantities through a functional relationship, where the uncertainty of output estimate or measurement result can be determined from the estimated standard deviation associated with each input estimate x_i , as shown in Equation (8)

$$u_c^2(nt) = \left[\frac{\partial f}{\partial \rho} \right]^2 u^2(\rho) + \left[\frac{\partial f}{\partial m} \right]^2 u^2(m) + \left[\frac{\partial f}{\partial d} \right]^2 u^2(d) + \left[\frac{\partial f}{\partial h} \right]^2 u^2(h) + \left[\frac{\partial f}{\partial h_1} \right]^2 u^2(h_1) + \left[\frac{\partial f}{\partial h_3} \right]^2 u^2(h_3) + \left[\frac{\partial f}{\partial h_2} \right]^2 u^2(h_2) + u^2(s) \quad (8)$$

where $u_c(n_t)$ is the combined standard uncertainty of output estimate n_t ; $\partial f/\partial x_i$ is the partial derivative (sensitive coefficient) with respect to input quantities X_i ($\rho, m, d, h, h_1, h_3, h_2$) of functional relationship f between measurand n_t and input quantities X_i on which n_t depends, $u(x_i)$ is the standard uncertainty of input estimated x_i that estimates input quantity X_i , $u(s)$ is the standard uncertainty of the measurement repeatability of output estimate n_t , equal to the experimental standard deviation of the mean n_t .

Detailed calculation steps and precautions, see “Guide to the Expression of Uncertainty in Measurement” [42]. The uncertainty of the total porosity of loose raw coal under each pressure was calculated by Equation (8). The results under 20 MPa were shown in Table 6.

Table 6. Summary of standard uncertainty components.

Standard Uncertainty Component $u(x_i)$	Source of Uncertainty	Value of Standard Uncertainty $u(x_i)$	Sensitive Coefficient: $c_i = \partial f/\partial x_i$	Component of $u_c(n_t)$: $u_i(n_t) = c_i u(x_i)$ (%)
$u(\rho)$	Instrument uncertainty ($\pm 0.03\%$ of the indication)	2.83×10^{-4} g/cm ³	0.14654	0.00438
	Measurement repeatability ($\pm 0.01\%$ of the indication)	4.15×10^{-5} g/cm ³		
$u(m)$	Instrument uncertainty (± 0.02 g)	0.0115 g	0.00111	0.00128
$u(d)$	Instrument uncertainty (± 0.002 cm)	0.00115 cm	0.09667	0.0869
	Measurement repeatability	0.00892 cm		
$u(h)$	Instrument uncertainty (± 0.002 cm)	0.00115 cm	0.00314	0.00286
	Measurement repeatability	0.00904 cm		
$u(h_1)$	Instrument uncertainty ($\pm 0.5\%$ of the indication)	0.00730 cm	0.00314	0.00229
$u(h_3)$		0.00154 cm		0.000484
$u(h_2)$		0.000427 cm		0.000134
$u(s)$	-	-	-	0.140

$$u_c^2(n_t) = \sum u_i^2(n_t) + u^2(s) = 2.74 \times 10^{-5}; u_c(n_t) = 0.17\%.$$

Although u_c can be universally used to express the uncertainty of a measurement result, it only corresponds to the standard deviation, and the measurement result $y \pm u_c$ represented by it has a low level of confidence. The additional measure of uncertainty that meets the requirement of providing an interval of the high level of confidence is termed expanded uncertainty and is denoted by U . The expanded uncertainty U is obtained by multiplying the combined standard uncertainty $u_c(y)$ by a coverage factor k : $U = k u_c(y)$.

Take $k = 2$, the corresponding level of confidence p is 95%, $U = k u_c(n_t) = 2 \times 0.17\% = 0.34\%$.

The uncertainty of the total porosity measurement of loose raw coal under 20 MPa is evaluated by using the expanded uncertainty. The measurement result is

$$n_t = 10.22\% \pm 0.34\%, p = 95\%$$

The expanded uncertainty of the total porosity measurement of loose raw coal under 5, 10, 15, and 25 MPa is 0.40%, 0.38%, 0.18%, and 0.36%.

Table 5 shows that the standard uncertainty of the measurement repeatability of output estimate $u(s)$ accounts for the vast majority (82%) in the combined standard uncertainty $u_c(n_t)$. The main sources of $u(s)$ are the randomness of the coal samples, and the measurement repeatability of the coal sample mass. The value of this part of the uncertainty can be reduced by increasing the number of repetitions of the measurements.

4.3. Engineering Significance, Novelty, Applicability, and Scalability of the Method

Using this experimental method, the value and variation of the total porosity of loose coal with different depths and different degrees of fragmentation can be estimated to provide data for field engineering.

The main novelty of this method is the following aspects: the extension of relationship between total porosity, true density, and bulk density to the total porosity test of the loose media under overburden pressure, the application of mechanical press to measure bulk density, the reverse loading and the record of rebound amounts during the bulk density measurement process.

This experimental method is mainly applicable to loose and broken deposition, especially for shallow loose deposits like sand and soil. The in situ stress that can be simulated in this method depends mainly on the maximum test force of the mechanical press.

Next, the accuracy of results can be improved by higher device performance and more pressure and displacement sensors. The relationship between temperature and the total porosity can be studied by using a thermally conductive mold. In addition, some devices can be added to study the pore distribution and permeability of loose media under overburden pressure.

5. Conclusions

The porosity of coal is very important in coal mining, such as for evaluating coal reservoirs and selection of grouting materials for reinforcement of coal roadways. This work has presented an experimental study on porosity characterization of loose coal media subjected to controlled overburden pressure. A new experimental method for such has been proposed, and the correlations between porosity and pressure and porosity and particle size have been examined. The main conclusions of this work are summarized below.

- (1) A new method for characterizing total porosity in loose media subjected to overburden pressure is proposed. It is based on the functional relationship between total porosity, true density, and bulk density.
- (2) After testing, the porosity of loose coal from the Guobei Coal Mine at 20 MPa in situ stress is found to be $\approx 10.22\%$. The total porosity experiences a downward trend as pressure increases for a fixed particle size, and the total porosity and pressure obey an attenuated exponential function. The decrease in total porosity with initial single particle sizes (0–2, 2–5, and 5–15 mm) is similar to that with increasing pressure, with steep curves of total porosity vs. pressure evident. There is reduction in the rate of total porosity decrease with increasing pressure with a mixed particle sizes.
- (3) At each selected pressure, the total porosity increases with increasing initial particle size (large initial particle size correspond to low degree of on-site coal fragmentation), and the total porosity and initial particle size obey a power function. The rate of total porosity increase becomes gradually reduced as particle size increases at higher stress levels. The curve of initial particle size vs. total porosity approximates a horizontal line when the pressure exceeds 20 MPa, and can thus be considered indicative of total porosity being insensitive to changes in initial particle size or the degree of on-site coal fragmentation.
- (4) When pressures are low (e.g., burial conditions are shallow), it is found that total porosity is greatly reduced and is highly sensitive to the increase in pressure. However, total porosity is less sensitive to pressure at higher stress levels (e.g., burial conditions are deep). The effect of particle size on the total porosity reduction rate in the loose coal is not significant irrespective of the pressure conditions (e.g., low or high). In general, the sensitivity of the total porosity to pressure is found to be significantly higher than sensitivity to particle size.

Author Contributions: All of the authors contributed extensively to the work. C.Z., N.Z., and D.Q. proposed key ideas. C.Z., N.Z., and D.Q. conceived and designed the experiment schemes. C.Z., D.Q., D.P., and Y.A. conducted the experiment. C.Z., D.Q., and D.P. analyzed the data. C.Z. wrote the paper. D.Q., D.P., Y.A., Y.Y., Z.X., and Y.W. modified the manuscript.

Funding: This work was financially supported by the National Natural Science Foundation of China (grant nos. 51704277 and 51674244), the Fundamental Research Funds for the Central Universities (grant nos. 2018QNA27, 2017CXNL01, and 2017CXTD02), the project funded by China Postdoctoral Science Foundation (grant no.

2017M621874), and a project Funded by the Priority Academic Program Development of Jiangsu Higher Education Institutions.

Acknowledgments: We are grateful to the staff at the Guobei coal mine for their assistance during the on-site sampling. We thank Warwick Hastie, from Liwen Bianji, Edanz Group China (www.liwenbianji.cn/ac), for editing the English text of a draft of this manuscript.

Conflicts of Interest: The authors declare no conflict of interest.

References

1. Zhao, P.N. *Loose Medium Mechanics*; Seismological Press: Beijing, China, 1995.
2. Fan, J.J.; Ju, Y.W.; Hou, Q.L.; Tan, J.Q.; Wei, M.M. Pore structure characteristics of different metamorphic-deformed coal reservoirs and its restriction on recovery of coalbed methane. *Earth Sci. Front.* **2010**, *17*, 325–335.
3. Curtis, M.; Ambrose, R.; Sondergeld, C. Structural Characterization of Gas Shales on the Micro and Nano-Scales. In Proceedings of the Canadian Unconventional Resources and International Petroleum Conference, Calgary, AB, Canada, 19–21 October 2010.
4. Sammartino, S.; Siitarikauppi, M.; Meunier, A.; Sardini, P.; Bouchet, A.; Tevissen, E. An Imaging Method for the Porosity of Sedimentary Rocks: Adjustment of the PMMA Method—Example of a Characterization of a Calcareous Shale. *J. Sediment. Res.* **2002**, *72*, 937–943. [[CrossRef](#)]
5. Hübner, W. Studying the pore space of cuttings by NMR and μ CT. *J. Appl. Geophys.* **2014**, *104*, 97–105. [[CrossRef](#)]
6. Krzyżak, A.T.; Kaczmarek, A. Comparison of the Efficiency of 1H NMR and μ CT for Determining the Porosity of the Selected Rock Cores. In Proceedings of the International Multidisciplinary Scientific Geoconference Green Sgem, Vienna, Austria, 11 November 2016.
7. Yao, Y.B.; Liu, D.M.; Cai, Y.D.; Li, J.Q. Advanced characterization of pores and fractures in coals by nuclear magnetic resonance and X-ray computed tomography. *Sci. Sin. Terrae* **2010**, *40*, 1598–1607. [[CrossRef](#)]
8. Andrew, M. Reservoir Condition Pore Scale Imaging of Multiphase Flow Using X-ray Microtomography. Ph.D. Thesis, Imperial College London, London, UK, 2014.
9. Menke, H.P.; Andrew, M.G.; Blunt, M.J.; Bijeljic, B. Reservoir condition imaging of reactive transport in heterogeneous carbonates using fast synchrotron tomography—Effect of initial pore structure and flow conditions. *Chem. Geol.* **2016**, *428*, 15–26. [[CrossRef](#)]
10. Andrew, M.; Menke, H.; Blunt, M.J.; Bijeljic, B. The imaging of dynamic multiphase fluid flow using synchrotron-based X-ray microtomography at reservoir conditions. *Transp. Porous Med.* **2015**, *110*, 1–24. [[CrossRef](#)]
11. Hu, X.; Liang, W.; Hou, S.J.; Zhu, X.G.; Huang, W.Q. Experimental study of effect of temperature and stress on permeability characteristics of raw coal and shaped coal. *Chin. J. Rock Mech. Eng.* **2012**, *31*, 1222–1229. [[CrossRef](#)]
12. Liu, X.J.; Gao, H.; Liang, L.X. Study of temperature and confining pressure effects on porosity and permeability in low permeability sandstone. *Chin. J. Rock Mech. Eng.* **2011**, *30*, 3771–3778.
13. Meng, Y.; Li, Z.P. Experimental study on the porosity and permeability of coal in net confining stress and its stress sensitivity. *J. China Coal Soc.* **2015**, *40*, 154–159. [[CrossRef](#)]
14. Tian, H.; Zhang, S.C.; Liu, S.B.; Ma, X.S.; Zhang, H. Parameter optimization of tight reservoir porosity determination. *Pet. Geol. Exp.* **2012**, 334–339. [[CrossRef](#)]
15. Chao, Z.M.; Wang, H.L.; Xu, W.Y.; Yang, L.L.; Zhao, K. Variation of permeability and porosity of sandstones with different degrees of saturation under stresses. *Chin. J. Rock Mech. Eng.* **2017**, *36*, 665–680. [[CrossRef](#)]
16. Dong, J.J.; Hsu, J.Y.; Wu, W.J.; Shimamoto, T.; Hung, J.H.; Yeh, E.C.; Wu, Y.H.; Sone, H. Stress-dependence of the permeability and porosity of sandstone and shale from TCDP Hole-A. *Int. J. Rock Mech. Min. Sci.* **2010**, *47*, 1141–1157. [[CrossRef](#)]
17. Tan, X.H.; Li, X.P.; Liu, J.Y.; Zhang, L.H.; Fan, Z. Study of the effects of stress sensitivity on the permeability and porosity of fractal porous media. *Phys. Lett. A* **2015**, *379*, 2458–2465. [[CrossRef](#)]
18. Meng, Y.; Li, Z.; Lai, F. Experimental study on porosity and permeability of anthracite coal under different stresses. *J. Pet. Sci. Eng.* **2015**, *133*, 810–817. [[CrossRef](#)]
19. Kong, Q.; Wang, H.L.; Xu, W.Y. Experimental study on permeability and porosity evolution of sandstone under cyclic loading and unloading. *Chin. J. Geotech. Eng.* **2015**, *37*, 1893–1900.

20. Jia, C.J.; Xu, W.Y.; Wang, H.L.; Wang, R.B.; Yu, J.; Yan, L. Stress dependent permeability and porosity of low-permeability rock. *J. Cent. South Univ.* **2017**, *24*, 2396–2405. [[CrossRef](#)]
21. Zheng, J.; Zheng, L.; Liu, H.H.; Ju, Y. Relationships between permeability, porosity and effective stress for low-permeability sedimentary rock. *Int. J. Rock Mech. Min. Sci.* **2015**, *78*, 304–318. [[CrossRef](#)]
22. Liu, J.J.; Liu, X.G. The effect of effective pressure on porosity and permeability of low permeability porous media. *J. GeoMech.* **2001**, *7*, 41–44. [[CrossRef](#)]
23. Wei, J.P.; Wang, D.K.; Wei, L. Comparison of permeability between two kinds of loaded coal containing gas samples. *J. China Coal Soc.* **2013**, *38*, 93–99. [[CrossRef](#)]
24. Yue, J.W.; Wang, Z.F. Imbibition characteristics of remolded coal without gas. *J. China Coal Soc.* **2017**, *S2*, 377–384. [[CrossRef](#)]
25. Zhu, C.Q.; Xie, G.X.; Wang, L.; Wang, C.B. Experimental study on the influence of moisture content and porosity on soft coal strength characteristics. *J. Min. Saf. Eng.* **2017**, 601–607.
26. Xu, J.; Lu, Q.; Wu, X.; Liu, D. The fractal characteristics of the pore and development of briquettes with different coal particle sizes. *J. Chongqing Univ.* **2011**, *9*, 81–89. [[CrossRef](#)]
27. Su, L.J.; Zhang, Y.J.; Wang, T.X. Investigation on permeability of sands with different particle sizes. *Rock Soil Mech. Rock Soil Mech.* **2014**, *35*, 1289–1294.
28. Yu, M.G.; Chao, J.K.; Chu, T.X. Experimental study on permeability parameter evolution of pressure-bear broken coal. *J. China Coal Soc.* **2017**, 916–922. [[CrossRef](#)]
29. Yu, B.Y.; Chen, Z.Q.; Wu, Y.; Zhang, S.B.; Yu, L.L. Experimental study on the seepage characteristics of cemented broken mudstone. *J. Min. Saf. Eng.* **2015**, 853–858. [[CrossRef](#)]
30. Yuan, C.F. Tectonically deformed coal and coal gas outburst. *Coal Sci. Technol.* **1986**, 32–33. [[CrossRef](#)]
31. Tang, Y.Y.; Tian, G.L.; Sun, S.Q.; Zhang, G.C. Improvement and perfect way for the classification of the shape and cause formation of coal body texture. *J. Jiaozuo Inst. Technol. Nat. Sci.* **2004**, 161–164. [[CrossRef](#)]
32. Zhang, H. One of Parameters Reflecting Coal Reservoir Permeability—Block Coal Rate. *Coal Geol. Explor.* **2001**, *6*, 21–22. [[CrossRef](#)]
33. Y Leon, C.A.L. New perspectives in mercury porosimetry. *Adv. Colloid Interface Sci.* **1998**, *76*, 341–372. [[CrossRef](#)]
34. Guo, X.; Yao, Y.; Liu, D. Characteristics of coal matrix compressibility: An investigation by mercury intrusion porosimetry. *Energy Fuel* **2014**, *28*, 3673–3678. [[CrossRef](#)]
35. *Methods for Determining the Physical and Mechanical Properties of Coal and Rock—Part 4: Methods for Calculating the Porosity of Coal and Rock*; GB/T 23561.4-2009; Standards Press of China: Beijing, China, 2009; p. 6.
36. Guo, D.Y.; Li, C.J.; Zhang, Y.Y. Contrast Study on Porosity and Permeability of Tectonically Deformed Coal and Indigenous Coal in Pingdingshan Mining Area, China. *Earth Sci. J. China Univ. Geosci.* **2014**, *39*, 1600–1606. [[CrossRef](#)]
37. Wang, C. Research on Characteristics and Applications of the Permeability of Loaded Coal Containing Gas. Master's Thesis, Henan Polytechnic University, Jiaozuo, China, 2014.
38. Yang, X.P. *Physical Mineral Processing*; Metallurgical Industry Press: Beijing, China, 2014.
39. Labani, M.M.; Rezaee, R.; Saeedi, A.; Al Hinai, A. Evaluation of pore size spectrum of gas shale reservoirs using low pressure nitrogen adsorption, gas expansion and mercury porosimetry: A case study from the Perth and Canning Basins, Western Australia. *J. Petrol. Sci. Eng.* **2013**, *112*, 7–16. [[CrossRef](#)]
40. Zhang, S.W.; Meng, Z.Y.; Guo, Z.F.; Zhang, M.Y.; Han, C.Y. Characteristics and Major Controlling Factors of Shale Reservoirs in The Longmaxi Fm, Fuling Area, Sichuan Basin. *Nat. Gas Ind.* **2014**, *34*, 16–24. [[CrossRef](#)]
41. Hodot, B.B. *Outburst of Coal and Coalbed Gas (Chinese Translation)*; China Coal Industry Press: Beijing, China, 1966; p. 318.
42. ISO (International Organization for Standardization). *Guide to the Expression of Uncertainty in Measurement*; ISO Tag4; ISO: Genève, Switzerland, 1995.
43. JCGM (Joint Committee for Guides in Metrology). *International Vocabulary of Metrology-Basic and General Concepts and Associated Terms (VIM)*; In BIPM: Sèvres, France, 2008.

